Phosphate Release and Force Generation in Cardiac Myocytes Investigated with Caged Phosphate and Caged Calcium
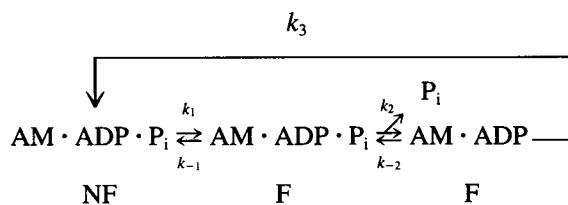
Alexandre Araujo and Jeffery W. Walker

Department of Physiology, University of Wisconsin, Madison, Wisconsin 53706 USA

ABSTRACT   The phosphate (P_i) dissociation step of the cross-bridge cycle was investigated in skinned rat ventricular myocytes to examine its role in force generation and Ca^{2+} regulation in cardiac muscle. Pulse photolysis of caged P_i (α-carboxyl-2-nitrobenzyl phosphate) produced up to 3 mM P_i within the filament lattice, resulting in an approximately exponential decline in steady-state tension. The apparent rate constant, k_{Pi}, increased linearly with total P_i concentration (initial plus photoreleased), giving an apparent second-order rate constant for P_i binding of 3100 M^{-1} s^{-1}, which is intermediate in value between fast and slow skeletal muscles. A decrease in the level of Ca^{2+} activation to 20% of maximum tension reduced k_{Pi} by twofold and increased the relative amplitude by threefold, consistent with modulation of P_i release by Ca^{2+}. A three-state model, with separate but coupled transitions for force generation and P_i dissociation, and a Ca^{2+}-sensitive forward rate constant for force generation, was compatible with the data. There was no evidence for a slow phase of tension decline observed previously in fast skeletal fibers at low Ca^{2+}, suggesting differences in cooperative mechanisms in cardiac and skeletal muscle. In separate experiments, tension development was initiated from a relaxed state by photolysis of caged Ca^{2+}. The apparent rate constant, k_{Ca}, was accelerated in the presence of high P_i, consistent with close coupling between force generation and P_i dissociation, even when force development was initiated from a relaxed state. k_{Ca} was also dependent on the level of Ca^{2+} activation. However, significant quantitative differences between k_{Pi} and k_{Ca}, including different sensitivities to Ca^{2+} and P_i, indicate that caged Ca^{2+} tension transients are influenced by additional Ca^{2+}-dependent but P_i-independent steps that occur before P_i release. Data from both types of measurements suggest that kinetic transitions associated with P_i dissociation are modulated by the Ca^{2+} regulatory system and partially limit the physiological rate of tension development in cardiac muscle.

INTRODUCTION

Cyclic interactions between myosin and actin produce force in muscle by coupling mechanical events with ATP splitting and sequential release of P_i and ADP. The P_i dissociation step of the muscle cross-bridge cycle is thought to be the chemical transition that is closest to the mechanical power stroke (Hibberd et al., 1985; Hibberd and Trentham, 1986), and the following kinetic model has been proposed (Dantzig et al., 1992):

$$
\begin{array}{ccccc}
& & k_3 & & \\
& & \uparrow & & \\
& k_1 & & k_2 & P_i \\
AM \cdot ADP \cdot P_i & \rightleftarrows & AM \cdot ADP \cdot P_i & \rightleftarrows & AM \cdot ADP \\
& k_{-1} & & k_{-2} & \\
NF & & F & & F
\end{array}
$$

Scheme 1

where A is actin, M is myosin, F is the force-generating states, NF is non-force states, and k_i are microscopic rate

constants. Studies of this process in isolated actomyosin in solution reveal a large free energy change and a P_i dissociation constant (k_2/k_{-2}) in the molar range (White and Taylor, 1976). This step may be better understood in muscle, where mechanical constraints imposed by the filament organization dramatically influence the thermodynamics of P_i dissociation (Pate and Cooke, 1989; Webb et al., 1986; Bowater and Sleep, 1988). Some of the free energy drop associated with the P_i release process is stored (or prevented from being released) during isometric contraction, and this creates a population of force-producing, ADP-bound bridges that are close enough in free energy to non-force-producing ADP·P_i-bound bridges that P_i can reverse force generation by simple mass action (Pate and Cooke, 1989; Dantzig et al., 1992). This apparent reversibility of the power stroke also identifies mechanical processes that are coupled to or rate-limited by P_i dissociation because they are sensitive to high P_i in the medium (Hibberd et al., 1985; Lu et al., 1993). This is due to the ability of P_i to displace the equilibrium toward P_i-bound states or to increase the pseudo-first-order P_i binding rate constant ($k_{-2}[P_i]$) and thus the rate of approach to a new steady state ($k_{-2}[P_i] + k_2$).

Kinetic properties of force transitions that are coupled to P_i dissociation have been investigated by photorelease of P_i within isometrically contracting skeletal fibers (Walker et al., 1992; Dantzig et al., 1992; Millar and Homsher, 1992). This has confirmed that force-producing transitions are readily reversible and closely associated with the P_i release

step in skeletal muscle. Rates are considerably faster than the steady-state ATPase rate, providing good evidence that the slowest step in the cycle follows P$_i$ release (Homsher and Millar, 1990). The process of force development after a period of unloaded shortening is also significantly slower than reversible force-generating transitions probed by caged P$_i$ photolysis (Millar and Homsher, 1990; Walker et al., 1992), showing that processes other than P$_i$ release may place limits on the physiological rate of force development. These measurements have also indicated that the caged P$_i$ tension transient in fast skeletal fibers is influenced in a characteristic way by variations in the level of Ca^{2+} activation (Walker et al., 1992), although the P$_i$ release process is not the main point in the cycle where Ca^{2+} regulation occurs (Millar and Homsher, 1990; Walker et al., 1992).

The present study was undertaken to investigate the P$_i$ release process in mammalian ventricular muscle. Although the cross-bridge cycle is likely to be similar in cardiac and skeletal fibers, specific kinetic transitions may differ. For instance, the P$_i$ release step may be slow enough in some fiber types, such as in insect flight muscle (Lund et al., 1987) and in slow (soleus) muscle (Millar and Homsher, 1992), to limit the rate of the ATPase reaction. It was of interest to determine whether the properties of mammalian ventricular muscle were more like slow muscles or like fast muscles, where P$_i$ release is measurably faster than ATPase and tension development rates.

It is also possible that regulation of the cross-bridge cycle by Ca^{2+} differs in cardiac and skeletal fibers. X-ray diffraction studies in cardiac muscle (Matsubara et al., 1989) have dissociated movement of cross-bridges toward the thin filament (which occurred at low Ca^{2+}) from force development (which occurred at higher Ca^{2+}). Thus, high Ca^{2+} might regulate force development by regulating the transition from an attached non-force-generating state to a force-generating state. Consistent with this idea, it has recently been shown that the rate of force development in cardiac muscle is Ca^{2+} dependent (Araujo and Walker, 1994; Wolff et al., 1995). Moreover, this Ca^{2+} dependence was found to be qualitatively and quantitatively different from that of fast skeletal fibers. Therefore, it was of interest to determine whether the P$_i$ release process was Ca^{2+} regulated in cardiac muscle.

The results show that P$_i$ influences cardiac myocyte contractility in a similar manner to what has been observed with fast skeletal fibers. The caged P$_i$ tension transient was four- to fivefold slower in cardiac myocytes than in fast skeletal fibers, but still faster than the tension development rate measured by photorelease of Ca^{2+} and faster than the ATPase rate. Variations in both Ca^{2+} and P$_i$ influenced the rate and amplitude of the caged P$_i$ tension transient, supporting previous data showing modulation of P$_i$ release by Ca^{2+} (Walker et al., 1992). Modeling using Scheme 1 accounted reasonably well for the effects of Ca^{2+} on the caged P$_i$ transient and was qualitatively consistent with the influence of P$_i$ on both caged Ca^{2+} tension transients and on the steady-state tension-pCa relationship. Finally, a large

thin filament inactivation process that complicated analysis of the caged P$_i$ transients in fast skeletal fibers was absent from cardiac myocytes, suggesting fundamental differences in how force-generating cross-bridges interact with thin filament regulatory proteins in skeletal and cardiac muscles.

MATERIALS AND METHODS

Caged P$_i$ was α-carboxyl-2-nitrobenzyl phosphate synthesized and purified as previously described (Walker et al., 1992). Caged Ca^{2+} (NP-EGTA; Ellis-Davies and Kaplan, 1994) was obtained from Molecular Probes (Eugene, OR).

Cardiac myocytes were prepared by brief homogenization of ventricles of female Sprague-Dawley rats as described previously (Araujo and Walker, 1994). Myocytes were skinned in 0.3% Triton X-100, 0.5% bovine serum albumin before attachment to the apparatus. Tension measurements in conjunction with flash photolysis were carried out using the apparatus described (Araujo and Walker, 1994). Attached myocytes averaged 150 μm long $\times$ 80 μm wide and probably represented bundles of 1–4 cells. Sarcomere length was set to 2.1–2.2 μm and monitored by video microscopy (Araujo and Walker, 1994). If sarcomere length decreased by more than 10% during activation, the data were not included in the data summary. All tension measurements were performed at 15°C.

Relaxing and activating solutions were of the following composition (in mM): 4 MgATP, 7.4 MgCl$_2$ (1 mM free Mg^{2+}), 7 EGTA, and 11 creatine phosphate. A computer program (Fabiato, 1988) was used to vary P$_i$, caged P$_i$, and free Ca^{2+} concentrations as well as the amount of KCl needed to maintain a constant ionic strength of 0.18 M. The stability constant for Ca^{2+} NP-EGTA was taken as 2 $\times$ 10^7 M^{-1} (Ellis-Davies and Kaplan, 1994).

Contaminating P$_i$, including that present in solutions and that produced by ATP hydrolysis in the cells, was assumed to be 0.7 mM (Walker et al., 1992). This could be reduced to 0.2 mM by incubation of solutions with 5 mM sucrose and 0.2 units/ml sucrose phosphorylase for 2 h (Pate and Cooke, 1989), which was kept in all solutions throughout the course of the experiment. The concentration of P$_i$ produced on photolysis was measured by irradiating test solutions containing various concentrations of caged P$_i$ in the 15-μl photolysis chamber. Photolyzed solutions were then assayed for free P$_i$ (Lanzetta et al., 1979). The amount of P$_i$ generated increased linearly with the initial concentration of caged P$_i$ up to 10 mM caged P$_i$. The slope of this line gave 25% photolysis per flash. Final P$_i$ concentrations were calculated as the sum of P$_i$ generated by photolysis and the P$_i$ that was present due to contamination of experimental solutions or to addition of P$_i$. Troponin C (TnC) extraction and recombination were carried out with the protocol described in Araujo and Walker (1994).

Data analysis and model simulations were carried out as described (Walker et al., 1992; Araujo and Walker, 1994). Tension traces were fit to single exponential functions using Marquardt's nonlinear regression algorithm and the following equations: P$_t$ = P$_{t=0}$(1 $-$ e^{-kt}) + mt, where m is the slope of the baseline; k = k_{Ca} for caged Ca^{2+} transients; k = k_{tr} for tension redevelopment transients; and for caged P$_i$ transients P$_t$ = P$_{t=0}$(e^{-kt}) + mt, where m is the slope of the baseline and k = k_{Pi}. Two criteria were used to evaluate the quality of fits: the standard error of the estimate of k value and the variance inflation factor (Glantz and Slinker, 1990), and the most appropriate equation was taken as the one that minimized these parameters. In many cases, the fits were significantly improved by eliminating the sloping baseline term (mt). Equations containing a sum of two exponentials were found to be unsuitable for fitting the tension traces, as standard errors of the estimates for k values were considerably larger than with single exponential fits and the variance inflation factor always increased, indicating that such equations were overparameterized. No delays of more than 2 ms were detected in the force development traces. Caged P$_i$ tension traces typically showed delays of 5–10 ms before force decline (Phase I of Dantzig et al., 1992), and these were not included in the fits. Amplitudes and rate constants for the caged P$_i$ tension transients were also obtained independently by an inspection

method. The amplitude was defined by a vertical line originating at the flash and intersecting a line that defined the baseline (see Figs. 1 A and 3 A). The rate constant was derived from $t_{1/2}$ (where $k = \ln 2/t_{1/2}$), which was determined by the time to one-half of the amplitude (illustrated in Figs. 1 A and 3 A). Values obtained for amplitudes and rate constants were within 15% using the various fitting procedures. Tension transients were collected at a sampling rate of 1 kHz. Unless otherwise stated, tension amplitudes are reported relative to P_o, the maximum tension at pCa 4.5 with no added P_i.

RESULTS

Fig. 1 A illustrates a representative tension transient that results from photorelease of 2.5 mM P_i in the filament lattice of an isometrically contracting skinned rat myocyte.
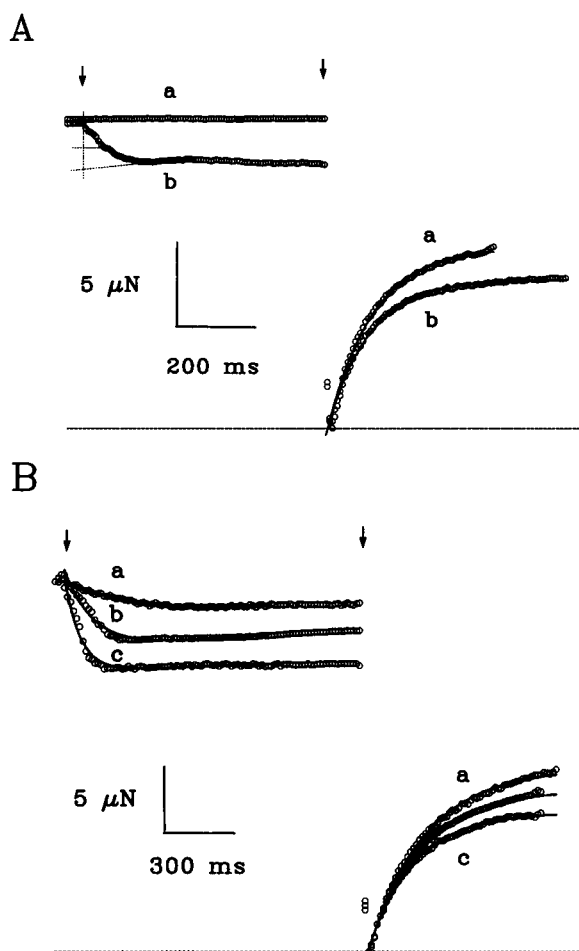

FIGURE 1 Representative original records of caged P_i tension transients in skinned cardiac myocytes. Attached myocytes were activated to a steady-state contraction, photolyzed by a single flash from a xenon lamp (first arrow), then released by a 10% length change (second arrow). Solid lines show fits to single exponential functions. (A) (a) No caged P_i; $k_{tr} = 5.6 \text{ s}^{-1}$. (b) 10 mM caged P_i, $k_{Pi} = 11.7 \text{ s}^{-1}$, amplitude = 15.4% P_o (where P_o is maximum tension under standard conditions, pCa 4.5, no added P_i), $k_{tr} = 6.2 \text{ s}^{-1}$. (B) Effects of varying [P_i]. Myocytes were incubated with sucrose/sucrose phosphorylase to reduce [P_i] to 0.2 mM before photolysis. In different trials, caged P_i concentration was varied while photolysis pulse intensity was constant. (a) 1 mM caged P_i, $k_{Pi} = 4.3 \text{ s}^{-1}$, amplitude = 6% P_o, $k_{tr} = 2.7 \text{ s}^{-1}$; (b) 3 mM caged P_i, $k_{Pi} = 6.2 \text{ s}^{-1}$, amplitude = 17% P_o, $k_{tr} = 3.0 \text{ s}^{-1}$; (c) 10 mM caged P_i, $k_{Pi} = 11.5 \text{ s}^{-1}$, amplitude = 25% P_o, $k_{tr} = 3.4 \text{ s}^{-1}$. Dotted lines indicate zero tension.

Only in the presence of caged P_i was there an abrupt tension decline on exposure to the near-UV light pulse. Pre-photolysis [P_i] was estimated to be 0.7 mM, and 2.5 mM was released from caged P_i. Fitting this and related transients to a single exponential function gave an apparent rate constant (k_{Pi}) of 11.6 ± 0.6 s^{-1} ($n = 105$) and an amplitude of 13 ± 2% P_o (P_o is the tension at pCa 4.5 without added P_i). In the protocol used, after 1 s myocyte length was released to allow assessment of total force as well as the ensuing tension redevelopment process. Typically, in skeletal fibers tension redevelopment (k_{tr}) is measured after a release, a period of shortening, and a restretch to the original sarcomere length (Brenner, 1988). In our experiments with cardiac myocytes, the restretch caused excessive rundown of force, and thus this maneuver was eliminated from the protocol. Therefore, tension redevelopment data presented here in cardiac myocytes must be interpreted with caution because redevelopment occurs at a shorter sarcomere length than the caged P_i transient. For this reason we also measured tension development by photolysis of caged Ca^{2+} (NP-EGTA; Ellis-Davies and Kaplan, 1994) as a more reliable and physiologically relevant tension development process (see below).

To further test whether the caged P_i tension transient was probing a reversible P_i release step in the cross-bridge cycle, the dependence on P_i concentration was evaluated. In Fig. 1 B, the attached cell and caged P_i solutions were preincubated with sucrose/sucrose phosphorylase to reduce the free [P_i] to 0.2 mM (Pate and Cooke, 1989) before photorelease of P_i. Both the rate and amplitude of the tension decline depended on the concentration of P_i released (Figs. 1 B and 2). The tension redevelopment process, k_{tr}, was also accelerated by higher P_i concentrations but overall was considerably slower than k_{Pi} (Fig. 2 A). The P_i dependence for k_{Pi} was linear, with an apparent second-order rate constant of 3100 $M^{-1} \text{ s}^{-1}$ (Fig. 2 A).

The amplitude of the tension decline after photorelease of 2.5 mM P_i was similar to the decline in steady-state tension observed in the presence of 2.5 mM P_i. Data obtained from caged P_i transient amplitudes and from the effects of added P_i on steady-state tension were approximately linear when plotted versus log [P_i] (Fig. 2 B), as has been shown in skeletal muscle fibers (Pate and Cooke, 1989; Millar and Homsher, 1990). Deviations from linearity, particularly at very low P_i, could be accounted for by a model that includes a two-step P_i release process, as in Scheme 1 (Dantzig et al., 1992). Because of uncertainties in the P_i concentration in this range and the fact that only one point deviated from the line (Fig. 2 B), this cannot be taken as evidence for two-step P_i release in cardiac myocytes. The values for constants in Scheme 1 obtained from data in Fig. 2 B also should be interpreted with caution. However, a related observation was made that treatment with sucrose/sucrose phosphorylase often had negligible effects on maximum tension in cardiac myocytes. A combination of the two-step mechanism and a low (>10 mM) P_i binding affinity provides a plausible explanation for this observation. Further experi-
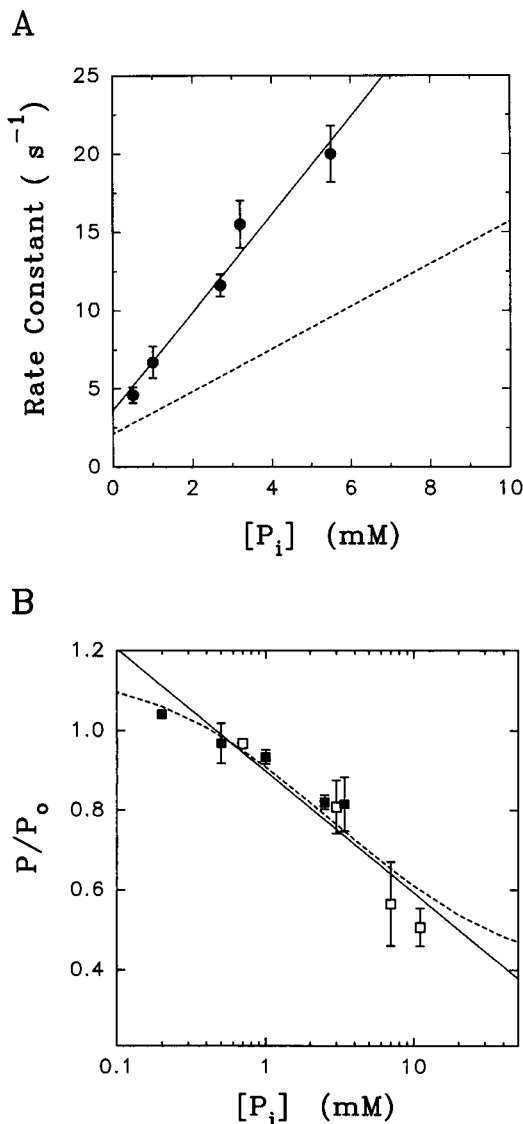
A

B

FIGURE 2   Summary of the influence of [P$_i$] on the rates and amplitudes of tension transients. (A) The observed rate constant for the caged P$_i$ tension transient, k_{P_i}, versus [P$_i$] (●). The solid line represents a linear regression fit with a slope of 3.1 mM^{-1} s^{-1}. The dotted line represents a linear regression fit to k_{tr} data for comparison (data points not shown for clarity). (B) Effects of [P$_i$] on the amplitude of the caged P$_i$ transient. Data from steady-state P$_i$ additions (□) and amplitudes of caged P$_i$ transients (■). Data are normalized to P/P$_o$ = 1.0 at 0.7 mM P$_i$ (without added P$_i$) or P/P$_o$ = 1.05 at 0.2 mM P$_i$ (in the presence of sucrose/sucrose phosphorylase). The solid line shows a linear regression fit with a slope of −0.366. The dotted line shows a fit to an equation derived from a two-step P$_i$ release model as in Scheme 1 (Dantzig et al., 1992): P/P$_o$ = α ln (1 + H((K_2 + k_3/k_{-2} + [P$_i$])/(K_2 k_3/k_{-1} + k_3/k_{-2} + [P$_i$]))) with α = 0.39, H = 7, K_2 = 15 mM, k_3 = 1.8 s^{-1}, k_{-2} = 40 mM^{-1} s^{-1}, and k_{-1} = 113 s^{-1}. Data are mean ± SEM for a minimum of four cells.
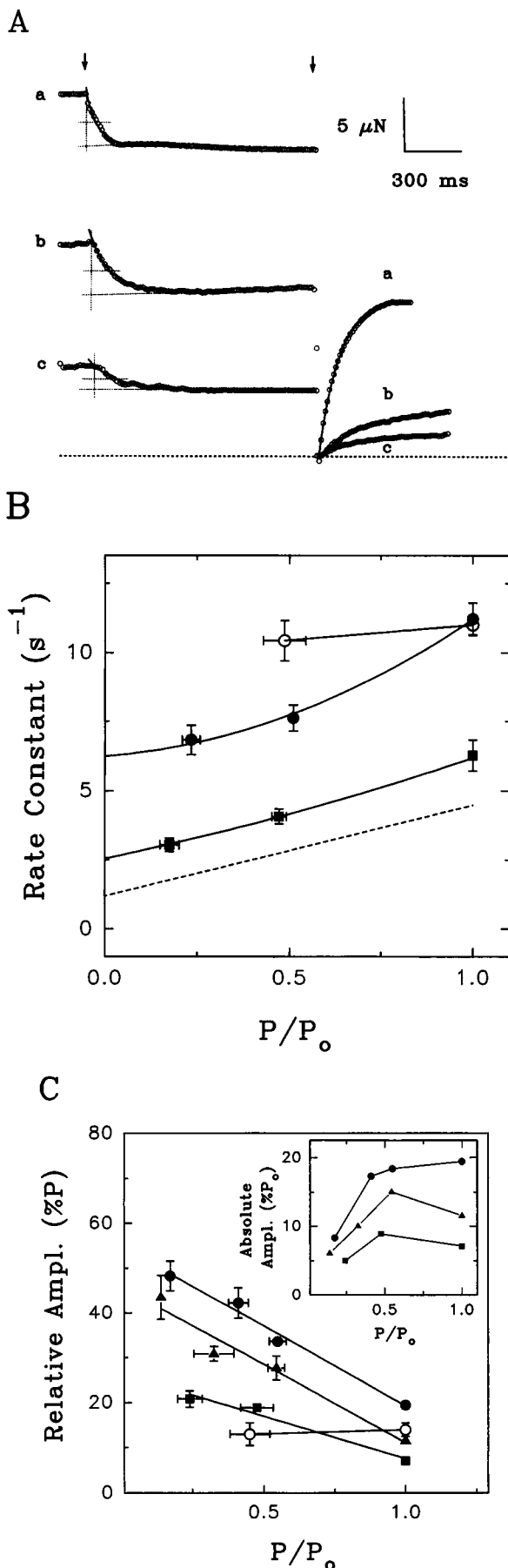
ments are required to establish a reliable value for the P$_i$ dissociation constant in this system, although the present data show that it is considerably greater than 6 mM.

The effects of varying the level of Ca^{2+} activation on the caged P$_i$ tension transient are shown in Fig. 3. One striking observation was that the transients were fit reasonably well

by single exponential terms at all levels of Ca^{2+}. This contrasts rather dramatically with rabbit psoas fibers, where at levels of Ca^{2+} activation below about 0.7 P$_o$ a slow phase of tension decline became apparent that typically was larger than the fast phase of tension decline (Walker et al., 1992). This made analysis of the caged P$_i$ transients at low Ca^{2+} much more straightforward in cardiac myocytes. At sub-maximum Ca^{2+}, the rate of the transient was slower by up to twofold (Fig. 3 B). Similar results were obtained when half-times for the tension transients were examined (see Materials and Methods), arguing against inexact curve fitting as the cause of this observation. A further indication that variations in Ca^{2+} significantly influenced the P$_i$ release process was that the amplitude of the caged P$_i$ tension transient reduced tension by a larger fraction as Ca^{2+} activation was reduced. This can be seen in the original records of Fig. 3 A, as transient b was the same size as transient a, even though the levels of Ca^{2+} and pre-photolysis tension were much lower in b. Another way to state the observation is that the amplitude of the caged P$_i$ transient did not scale with the pre-photolysis tension but was larger in relative terms at low Ca^{2+}. The data are summarized for three different levels of photoreleased P$_i$ in Fig. 3 C, plotted as relative amplitude to facilitate comparison with previous work (Walker et al., 1992; Millar and Homsher, 1990). No effect of Ca^{2+} on relative amplitude would give horizontal lines in this plot. To facilitate modeling (see below), the same data were plotted as absolute amplitude (Fig. 3 C, inset), which would give straight, upward-sloping lines beginning at zero if Ca^{2+} had no effect. Thus, although the influence of Ca^{2+} on k_{P_i} is relatively modest, it is consistent with the effects of Ca^{2+} on amplitude and can be explained by a simple model (Fig. 7).

The effects of variation in Ca^{2+} activation appear to be specific for Ca^{2+}, as reducing tension by partial extraction of TnC did not cause the same changes in rate (Fig. 3 B) and amplitude (Fig. 3 C) of the transients. After TnC removal to reduce tension at pCa 4.5 to approximately 50% P$_o$, the rate was unaffected by the reduction in tension alone, and the amplitude scaled with tension (Figs. 3 B and C, open symbols).

Another series of experiments was carried out in which force development rates were measured after photorelease of Ca^{2+}. Beginning from a relaxed state, a single near-UV light pulse initiated an approximately exponential tension increase to different levels of tension, depending on the amount of Ca^{2+} released (Fig. 4). In these experiments, the fastest tension development process occurred with k_{Ca} of 3.9 s^{-1}, and the final tension level was 93% P$_o$. Lower levels of activation achieved by reducing the Ca^{2+} load of NP-EGTA gave slower tension development; for example, k_{Ca} was 0.6 s^{-1} at a final tension of 15% P$_o$ (Fig. 4 A). At all levels of Ca^{2+} released from NP-EGTA, the tension transients were fit adequately by a single exponential term. Single exponentials with sloping baselines or double exponentials did not fit the data better, as judged by visual inspection and by minimizing the standard error of the estimated k_{Ca} value and

A

5 μN

300 ms

B

Rate Constant (s^{-1})

P/P$_o$

C

Relative Ampl. (%P)

Absolute Ampl. (%P$_o$)

P/P$_o$

P/P$_o$

minimizing the variance inflation factor (see Materials and Methods). A summary of the effects of variation in the level of Ca^{2+} activation on the rate of tension development is given in Fig. 4 B. From these data it is clear that k_{Ca} increases about fivefold when Ca^{2+} is varied over the range that supports isometric tension, corroborating earlier studies with a different caged Ca^{2+}, Nitr-7, that detected a fourfold increase (Araujo and Walker, 1994).

The effects of P_i on the caged Ca^{2+} tension transient were also examined. Inclusion of 10 mM P_i in the photolysis solution accelerated k_{Ca} by about threefold, similar in behavior to tension redevelopment measured in each trace after release of the cell length, i.e., k_{tr} (Fig. 5 B). The rate constant, k_{Ca}, for the Ca^{2+}-initiated transient was 3.8 ± 0.3 ($n = 58$) at 0.7 mM P_i and 9.5 ± 1.2 ($n = 11$) at 10.7 mM P_i, giving a second-order rate constant for P_i binding of 820 $M^{-1} s^{-1}$ (Fig. 5 B).

Steady-state tension-pCa measurements also provided evidence that Ca^{2+} and P_i interact to influence the tension development process. High P_i is known to reduce the apparent Ca^{2+} sensitivity of tension development in both skeletal and cardiac fibers (Kentish, 1986; Millar and Homsher, 1990; Palmer and Kentish, 1994). In ventricular myocytes, 10 mM P_i caused a rightward shift of the steady-state tension-pCa relationship by 0.28 pCa units, but there was no detectable change in the steepness, as assessed by the Hill coefficient (Fig. 6). Working with fast skeletal fibers, Millar and Homsher (1990) observed a large increase in the Hill coefficient in addition to the rightward shift in the presence of high P_i and proposed that this was related to the effects of submaximum Ca^{2+} on the amplitude of the caged P_i tension transient. Walker et al. (1992) proposed that the large slow thin filament inactivation process observed at low Ca^{2+} was responsible for the increase in the Hill coefficient at high P_i. In support of the latter view, ventric-

FIGURE 3 Effects of variation in the level of Ca^{2+} activation on the caged P_i transient. Attached myocytes were contracted to a steady state in the presence of 10 mM caged P_i and various levels of Ca^{2+}. Photolysis was initiated (*left arrow*), then the cell was released (*right arrow*). (*a*) pCa 4.5, $k_{Pi} = 12.1 s^{-1}$, amplitude = 12% P_o, $k_{tr} = 6.2 s^{-1}$. (*b*) pCa 5.5, $k_{Pi} = 6.7 s^{-1}$, amplitude = 10% P_o, $k_{tr} = 3.3 s^{-1}$. (*c*) pCa 5.7, $k_{Pi} = 5.4 s^{-1}$, amplitude = 6% P_o, $k_{tr} = 3.0 s^{-1}$. The dotted line indicates zero tension. (*B*) Summary of the effects of Ca^{2+} on k_{Pi}. The level of Ca^{2+} activation is indicated on the abscissa as the fraction of maximum tension developed (P/P_o) just before photolysis. Solid lines only serve to differentiate data sets. ■, 1 mM caged P_i, 0.5 mM P_i final; ●, 10 mM caged P_i, 2.7 mM P_i final. The dotted line indicates activation dependence of k_{tr} at 2.7 mM P_i measured sequentially in the same experiment (data omitted for clarity). Control experiment showing effects of reducing maximum tension by partial extraction of TnC: ○, 10 mM caged P_i, 2.7 mM final P_i, pCa 4.5. (*C*) Variation in amplitude of caged P_i transient with variation in Ca^{2+} activation. The ordinate represents the relative amplitude of the transient, i.e., the percentage decline of the pre-photolysis tension (%P). ■, 1 mM caged P_i, 0.5 mM final P_i; ▲, 3 mM caged P_i, 1 mM final P_i; ●, 10 mM caged P_i, 2.7 mM final P_i. Effects of TnC extraction at pCa 4.5: ○, 10 mM caged P_i. The absolute amplitude of the transient, i.e., the percentage decline normalized to maximal tension (%P$_o$), is also plotted (*inset*). Data are mean ± SEM for a minimum of four cells.
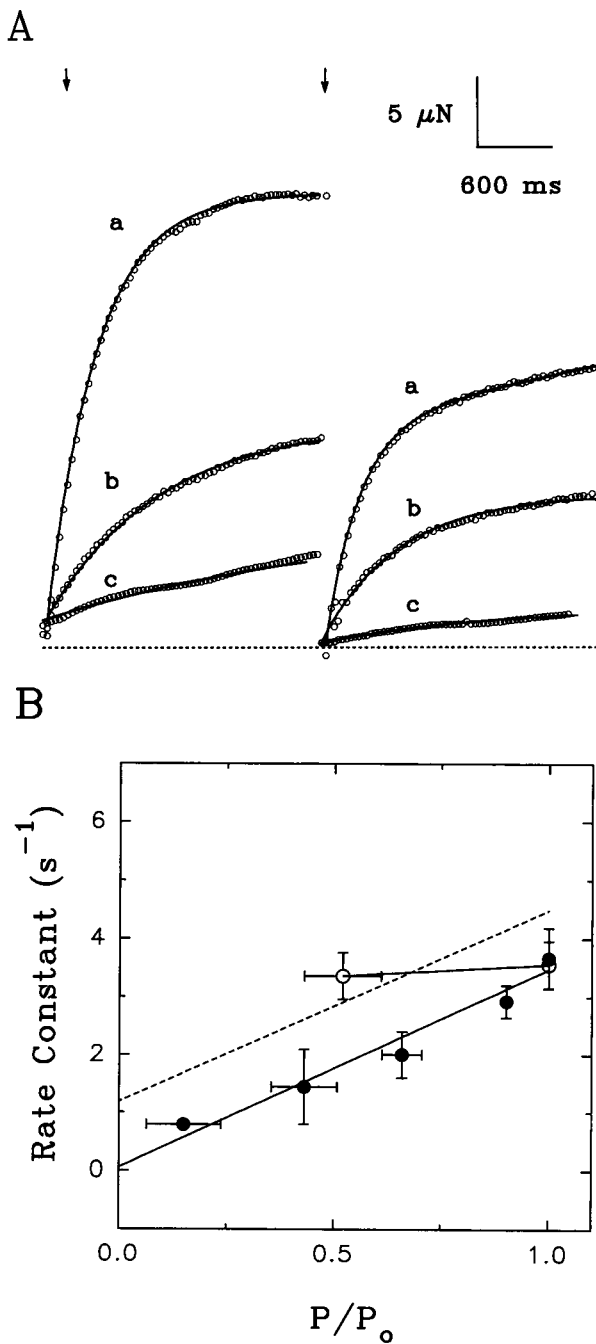
A

B

P/P$_o$

FIGURE 4   Effects of variation in Ca^{2+} on the caged Ca^{2+} tension transient. (A) Original records of an attached myocyte incubated in 1 mM P$_i$ plus 1 mM NP-EGTA loaded to different extents with Ca^{2+} and photolyzed (left arrow) with a fixed-intensity, near-UV light pulse. After 2 s (right arrow) the cell was released by a 10% length change. (a) NP-EGTA 90% loaded with Ca^{2+}, k_{Ca} = 3.9 s^{-1}, amplitude = 93% P$_o$, k_{tr} = 3.7 s^{-1}. (b) NP-EGTA 82% loaded with Ca^{2+}, k_{Ca} = 1.3 s^{-1}, amplitude = 36% P$_o$, k_{tr} = 1.8 s^{-1}. (c) NP-EGTA 73% loaded with Ca^{2+}, k_{Ca} = 0.57 s^{-1}, amplitude = 15% P$_o$, k_{tr} = 0.9 s^{-1}. The dotted line shows zero tension. (B) Summary of effects of Ca^{2+} on k_{Ca}. The level of Ca^{2+} activation is indicated on the abscissa as the fraction of maximum tension developed (P/P$_o$) just before the length release. The solid line shows a linear regression fit. The dotted line illustrates the activation dependence of k_{tr} measured sequentially in the same experiment. Data are mean ± SEM for nine cells. O, Control experiment showing effects of TnC extraction on NP-EGTA transient 90% loaded with Ca^{2+}.
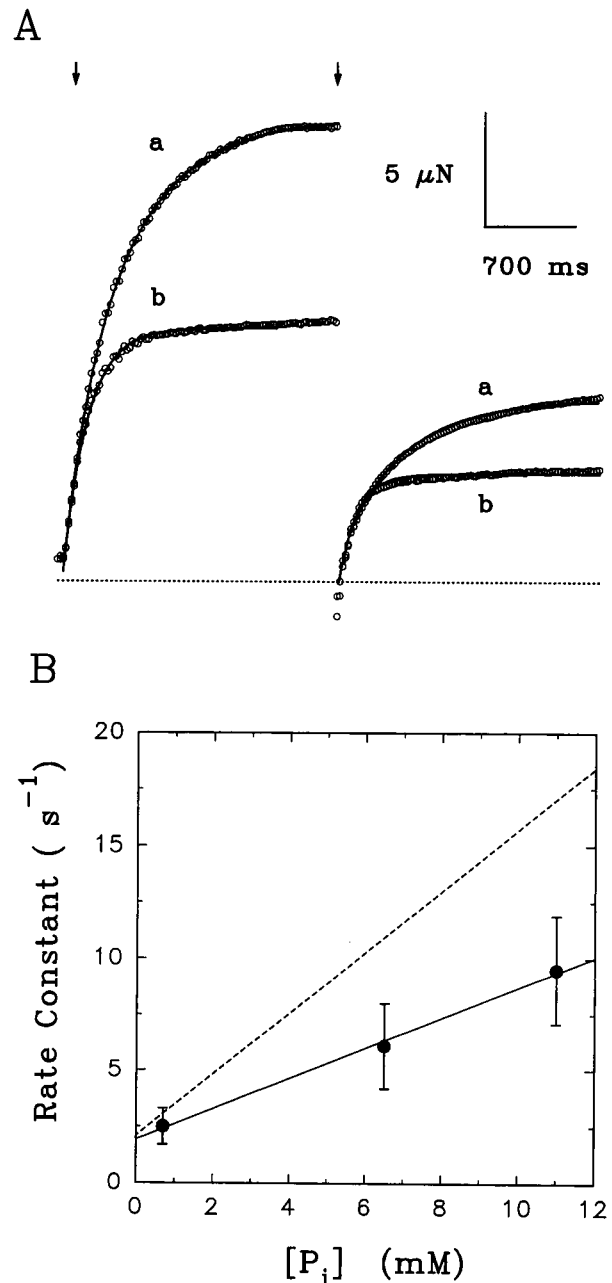
A

B

[P$_i$]   (mM)

FIGURE 5   Effects of P$_i$ on tension development after photorelease of Ca^{2+} from NP-EGTA. (A) Original records of a relaxed cell incubated with 1 mM Ca^{2+}-loaded NP-EGTA was exposed to a near-UV light pulse (left arrow), then released by 10% of its length (right arrow). (a) No added P$_i$, k_{Ca} = 3.4 s^{-1}, amplitude = 90% P$_o$, k_{tr} = 3.7 s^{-1}. (b) 10 mM added P$_i$, k_{Ca} = 7.3 s^{-1}, amplitude = 44% P$_o$, k_{tr} = 11.4 s^{-1}. The solid lines show fits to single exponentials. The dotted line shows zero tension. (B) Summary of [P$_i$] dependence of k_{Ca}. The solid line represents a linear regression with a slope of 0.82 mM^{-1} s^{-1}. The dotted line illustrates the P$_i$ dependence of k_{tr} for comparison. Data are mean ± SEM for four cells.

ular myocytes that displayed no change in the Hill coefficient in the presence of 10 mM P$_i$ (Fig. 6) also showed no slow phase of tension decline (Fig. 3 A), while retaining the effects of Ca^{2+} on relative caged P$_i$ amplitude (Fig. 3 C). Both the caged P$_i$ tension transient at low Ca^{2+} and the
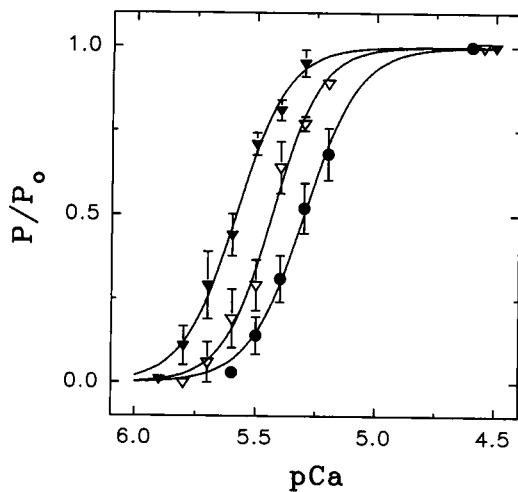
FIGURE 6   Effects of P_i on the steady-state tension versus pCa relationship in cardiac myocytes. The solid curves show fits to the Hill equation: $P/P_o = [Ca^{2+}]^{nH}/([Ca^{2+}]^{nH} + K^{nH})$, where n_H is the Hill coefficient and K is the apparent dissociation constant for Ca^{2+}. $K = 10^{-pCa50}$, where pCa_{50} is the pCa value that gives 50% of maximum tension. Maximum tension for each data set was normalized to the tension observed at pCa 4.5 at the $[P_i]$ used. ▼, Sucrose/sucrose phosphorylase, $[P_i] = 0.2$ mM, $n_H = 4$, $pCa_{50} = 5.58$, $P_{[0.2]}/P_o = 1.0$. ▽, 3 mM $[P_i]$ added, $n_H = 4.3$, $pCa_{50} = 5.43$, $P_{[3.7]}/P_o = 0.78$. ●, 10 mM $[P_i]$ added, $n_H = 3.8$, $pCa_{50} = 5.30$, $P_{[10.7]}/P_o = 0.52$.

FIGURE 7   Simulations of Scheme 1. To account for interactions between Ca^{2+} and P_i, k_1, which defines the probability of the forward NF to F transition, was assumed to increase from 0.25 s^{-1} to 5 s^{-1} with Ca^{2+}. $k_{-1}k_{-2}/k_2 = 3$ mM^{-1} s^{-1} was taken from the P_i concentration dependence (Fig. 2 A). (A) Simulation of the P_i dependence. (B) Simulation of the Ca^{2+} sensitivity of k_{Pi} at 0.5 mM P_i (solid line), 1 mM P_i (long dashes), and 3 mM P_i (short dashes). (C) Simulation of the Ca^{2+} sensitivity of the absolute amplitude of the caged P_i transient at the same three P_i concentrations used in B. (D) Simulation of tension-pCa curves at 0.2 mM P_i (solid line) and 10 mM P_i (long dashes).

effects of high P_i on the steady-state tension-pCa relationship are clearly different in ventricular myocytes compared with fast skeletal fibers (Millar and Homsher, 1990; Walker et al., 1992).

In fast skeletal fibers the apparent saturation of the rate of the caged P_i transient permitted the rate constants to be derived for a two-step model, as in Scheme 1. If a similar two-step P_i release mechanism exists in cardiac myocytes, and the binding of P_i (Step 2) is assumed to equilibrate more rapidly than Step 1, then k_1 can be estimated from the y-intercept of Fig. 2 A, because $k_{Pi} = k_1 + k_{-1}[P_i]/(K_2 + [P_i])$. k_1 estimated in this way is 4–5 s^{-1}. k_{-1} cannot be determined explicitly because it is defined by the rate at saturating P_i ($k_{Pi\ max} = k_1 + k_{-1}$), and no saturation was observed. However, k_{-1} has to be at least 20 s^{-1} to account for the fivefold increase in k_{Pi} at high P_i levels (Fig. 2 A). Values for the kinetic constants k_{-1}, k_2, and k_{-2} in Fig. 7 were constrained by the P_i dependence of k_{Pi} (Fig. 2 A) such that $k_{-1}k_{-2}/k_2 = 3$ mM^{-1} s^{-1}. The behavior of the model was not highly dependent upon the precise values chosen for these three constants. The Ca^{2+} dependence of the rate and amplitude of the caged P_i transient is best explained by assuming that k_1 varies from 0.25 s^{-1} to 5 s^{-1} over the physiological range of Ca^{2+}. As shown in Fig. 7, this accounts at least qualitatively for all of the fundamental observations, including the slowing of k_{Pi} at reduced levels of Ca^{2+} activation (Fig. 7 B), the nonlinear absolute caged P_i amplitude (Fig. 7 C), and the rightward shift of the tension-pCa curve in the presence of 10 mM P_i (Fig. 7 D). The predicted shift of 0.1 pCa unit with 10 mM P_i was
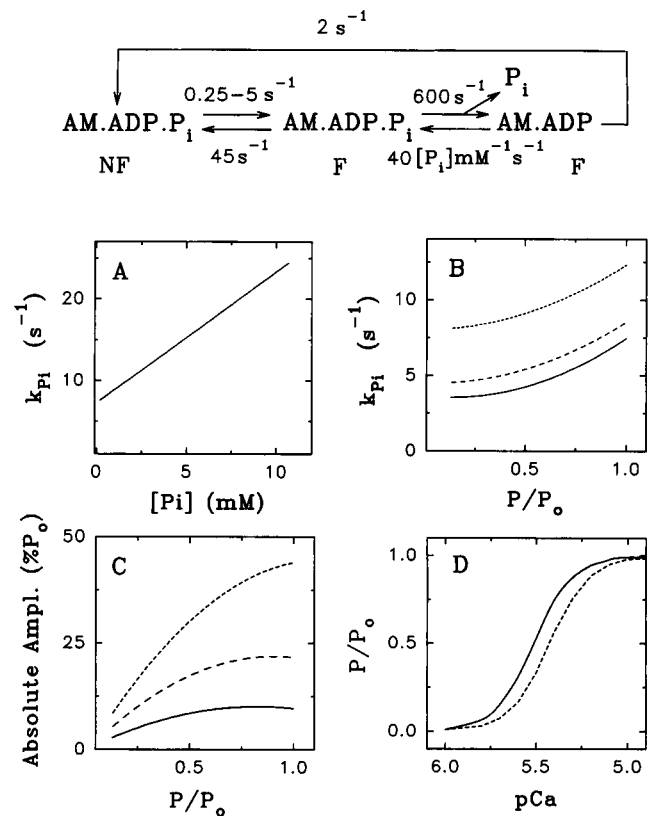
about 36% of the observed shift of 0.28 pCa unit (Fig. 6). The Ca^{2+} dependence of k_1 makes the equilibrium constant for the force-generating transition (NF to F) Ca^{2+} dependent and has the beneficial effect of shifting the steady-state distribution of cross-bridges toward force-generating states at high Ca^{2+} (Walker et al., 1992). No other rate constant in Scheme 1 when made Ca^{2+}-sensitive had the same effects on the behavior of the system. For example, whereas varying k_3 with Ca^{2+} influenced the simulated k_{Pi} appropriately and contributed to the P_i-induced rightward shift of the tension-pCa curve, changes in the absolute amplitude of the caged P_i transient were the complete opposite of what was observed in Fig. 3 C, inset. A limitation of the modeling was that simulations of Scheme 1 predicted that k_{Ca} and k_{Pi} would have essentially the same rate and dependencies on Ca^{2+} and P_i, and this was not observed experimentally. Thus, although Scheme 1 explains the caged P_i tension transients, it must be modified to accommodate the properties of the caged Ca^{2+} tension transients.

DISCUSSION

The results of this study show that rapid elevation of P_i within the filaments of skinned cardiac myocytes reduces contractile force in a manner that is consistent with coupling of a reversible P_i release process with a reversible force-generating transition. High P_i in the medium also accelerated tension development initiated by a Ca^{2+} jump, consistent with kinetic coupling between P_i release and tension development from a relaxed state. P_i release probably partially limits the rate of tension development in cardiac myocytes.

Kinetics of P_i release in cardiac muscle

Both the rate and amplitude of the force decline after a P_i jump were dependent upon the concentration of P_i, giving a second-order rate constant for P_i binding of $3100\ M^{-1}\ s^{-1}$. This rate constant is too slow to represent formation of the P_i:cross-bridge collision complex but probably reflects P_i binding and a rapid conformational change ($k_{-1}k_{-2}/k_2$ in Scheme 1). This conformational change in force-generating cross-bridges occurred about 5 times slower in cardiac myocytes than in fast skeletal fibers (Walker et al., 1992) and about 6 times faster than in slow skeletal fibers (Millar and Homsher, 1992), and thus appears to be related to the isoform of myosin present. No deviation from linearity or apparent saturation of the rate was observed in the P_i dependence, which is different from what was observed in fast skeletal muscle (Dantzig et al., 1992; Walker et al., 1992; Kawai and Halvorsen, 1991). A reasonable explanation for this result and the modest effects of sucrose/sucrose phosphorylase treatment on steady-state force in cardiac myocytes is that P_i binds with lower affinity in cardiac muscle than in fast skeletal muscle. Kawai et al. (1993) reported a threefold lower P_i affinity in ferret trabeculae compared with rabbit psoas fibers.

These direct perturbations of the P_i release process in cardiac myocytes show that this step in the cross-bridge cycle is much faster than the steady-state rate of ATP hydrolysis, which is measured to be $0.4\ s^{-1}$ in guinea pig trabeculae (Barsotti and Ferenczi, 1989). Thus, cardiac myocytes are different in this respect from slow skeletal and insect flight muscles. Because the P_i release rate is faster than the steady-state ATPase rate, ADP-bound states (rather than ADP·P_i-bound states) are likely to be the predominant force-producing states in contracting cardiac muscle. Further consideration of state distributions shows that k_1/k_{-1}, which is important in defining the distribution of cross-bridges between force-generating and non-force-generating states, is smaller than 0.2 in cardiac myocytes. The value for k_1/k_{-1} previously obtained in fast skeletal muscle was 0.24 (Walker et al., 1992) and indicates that in both muscle types, this step substantially favors non-force-generating states.

The effects of P_i on steady-state tension were similar in cardiac and fast skeletal muscle, as judged by the slope of the log $[P_i]$ versus tension plot, which was -0.366 in

cardiac fibers (Fig. 2 B) and -0.320 in fast skeletal fibers (Millar and Homsher, 1992). Thus, in terms of the sensitivity of different fiber types to P_i build-up, cardiac and fast skeletal fibers appear to be similar, except at very low P_i concentrations. By contrast, slow skeletal fibers, which are known to be fatigue resistant and P_i insensitive, displayed a much smaller slope (-0.19) of this $log[P_i]$ versus tension relationship (Millar and Homsher, 1992).

Effects of Ca^{2+}

The effects of variation in the level of Ca^{2+} activation on the caged P_i tension transient are modest, and we conclude that the Ca^{2+} regulatory system has at best a modulatory influence on the kinetics of P_i release in cardiac muscle. The slowing of the kinetics of P_i release at low Ca^{2+} do appear to be specific for Ca^{2+}, because a similar reduction in tension by TnC removal had no effects on the rate and amplitude of the transient. Scheme 1, which contains separate but coupled transitions for force generation and P_i dissociation, can account for the observed changes with Ca^{2+} if the forward rate constant for force generation is Ca^{2+} dependent (see Fig. 7). The effect of high Ca^{2+} on this step in the cycle promotes force generation as it shifts the equilibrium between non-force and force states toward force states. Because the rate of flux through this state in the cycle is approximately the sum of forward and reverse rate constants and because the reverse rate constant is much larger than the forward, the effects of Ca^{2+} on the rate of flux through this step are small and in fact somewhat difficult to detect (Fig. 3, A and B). Ca^{2+} effects on the ratio of forward and reverse rate constants is more dramatic and is readily detected as a change in relative amplitude of the transient (Fig. 3 C). An important general conclusion is that the P_i release process is not the main control point for Ca^{2+} regulation of the cross-bridge cycle, although it may account for as much as 40% of the Ca^{2+} sensitivity of the rate of tension development in cardiac muscle (see below). A similar conclusion has been reached in studies of fast skeletal muscle (Millar and Homsher, 1990; Walker et al., 1992), although there Ca^{2+} modulation of P_i release accounted for less than 20% of the Ca^{2+} sensitivity of tension development rate.

Relationship between k_{Ca} and k_{Pi}

A comparison of the caged P_i and caged Ca^{2+} transients reveals qualitative similarities, including both being accelerated by Ca^{2+} and by high P_i. However, quantitative differences were significant. k_{Pi} was two- to threefold faster than corresponding k_{Ca} values at similar P_i concentrations (compare Figs. 2 A and 5 B). Values for k_{tr} were intermediate between k_{Pi} and k_{Ca}; but k_{tr} values were generally more variable, and we consider k_{tr} measurements to be useful mainly as an internal reference that facilitated comparison of the other two types of transients. In sequential measure-

ments over a range of P_i concentrations, k_{P_i} was always faster than k_{tr} (Fig. 2 A), whereas k_{Ca} was always slower than k_{tr} (Fig. 5 B), and the slopes of the P_i dependencies of k_{P_i} and k_{Ca} were different by a factor of 3.8. Conversely, k_{Ca} increased fivefold over the range of Ca^{2+} that supported isometric tension (Fig. 4 B), whereas k_{P_i} increased only twofold over a similar Ca^{2+} range (Fig. 3 B), clearly showing differences in the Ca^{2+} dependencies of the tension transients. This could be due to the fact that other Ca^{2+}-dependent but P_i-independent processes such as thin filament activation (i.e., troponin-tropomyosin movement), cross-bridge attachment, or other steps in the cross-bridge cycle contribute to limiting the rate of force development (k_{Ca}) and minimizing its P_i dependence. Likewise, k_{P_i} probably more directly probes a reversible P_i release process and is somewhat removed from Ca^{2+}-dependent events that precede it. A precise quantitative relationship between k_{P_i} and k_{Ca} must await transient kinetic measurements with rigorous sarcomere length control. However, it is unlikely that end compliance in the preparation is solely responsible for observed differences between k_{P_i} and k_{Ca}, as we found the ratio of k_{Ca} to k_{P_i} to be fairly constant regardless of the amount of compliance assessed by video analysis of sarcomere length (Araujo and Walker, 1994). Moreover, a decrease in tension at maximum Ca^{2+} achieved by partial extraction of TnC showed little change in the k_{P_i}/k_{Ca} ratio. A theoretical analysis of the influence of series elasticity on tension transients concluded that caged P_i transients and force development would be slowed in a similar manner by end compliance (Luo et al., 1993).

One important possibility is that caged P_i and caged Ca^{2+} tension transients have distinct properties because they probe populations of cross-bridges with different average strain. Because strain can influence the thermodynamics of state transitions (and presumably their kinetics), it is worth considering whether Scheme 1 could account for both types of tension transients if the effects of cross-brdige strain are included. Theoretical analyses indicate that P_i perturbs cross-bridges that are more highly strained than the average (Bowater and Sleep, 1988; Webb et al., 1986; Pate and Cooke, 1989). For the purpose of discussion we assume that cross-bridge strain will influence only the force-generating transition (NF to F in Scheme 1), and that strain will reduce the equilibrium constant (k_1/k_{-1}) for this transition either by reducing k_1 or increasing k_{-1}. The simplest way to make Scheme 1 fit the caged Ca^{2+} data better is to reduce the value of k_{-1} by an order of magnitude. This reduces the rate of flux through these steps, reduces the effects of high P_i, and increases the effects of Ca^{2+} on kinetics. Thus, Scheme 1 can be made to account for both caged P_i and caged Ca^{2+} data better if k_{-1} is made strain dependent, such that its value is 45 s^{-1} for the distribution of strains probed by a P_i jump, and 4.5 s^{-1} for the distribution of strains detected by a Ca^{2+} jump. However, the available evidence on the influence of cross-bridge strain suggests that most of the strain dependence is in the forward rate constant (i.e., k_1) (Huxley and Simmons, 1971; Dantzig et al., 1992). Inclu-

sion of strain dependence only in the forward rate constants (k_1 and/or k_2) in Scheme 1 causes simulated caged Ca^{2+} transients to be faster than simulated caged P_i transients (Song et al., 1996), and the model gives an even less satisfactory account of the data. Thus, when strain-dependent forward rate constants are included, it becomes even more necessary to add a slow Ca^{2+}-dependent step (e.g., cross-bridge attachment or tropomyosin movement) before Step 1 in Scheme 1.

To account for all of our results on Ca^{2+} modulation of kinetics in cardiac myocytes it is necessary to assign Ca^{2+} dependence to at least two processes: k_1 in Scheme 1 and steps that precede k_1 (not shown in Scheme 1). Ca^{2+} regulation of stiffness in the presence of ATP(γS) is consistent with Ca^{2+} regulation of early steps in the cross-bridge cycle that precede force generation and P_i release (Dantzig et al., 1988).

Cooperativity

A large slow component of tension decline was not observed in the caged P_i tension transients in cardiac myocytes. This component, previously observed in fast skeletal fibers, was interpreted as a cooperative thin filament inactivation phenomenon (Walker et al., 1992). As the number of attached cross-bridges is reduced by lowering the level of Ca^{2+} activation, elevation of P_i not only reverses the power stroke but also further reduces attached cross-bridges (Dantzig et al., 1992). With reduced numbers of bound cross-bridges cooperating to maintain an active state of the thin filament regulatory system, that system slowly inactivates at a rate that is presumably limited by cross-bridge reattachment and cycling. The reason why this phenomenon does not occur in cardiac myocytes must be related to the nature of interactions between cross-bridges and the regulatory system. One possibility is that cross-bridges function more independently in cardiac muscle and are less interactive with other cross-bridges on the thin filament strand. In this way, rapid P_i elevation will only perturb isolated cross-bridges and not precipitate a global cooperative phenomenon. This view is compatible with the approximately linear relationship between activation level and rate of tension development (Araujo and Walker, 1994; Fig. 4 B), which also suggests independent (graded) regulation of force-generating units. Another possibility is that interactions between cross-bridges and the thin filament are more extensive in cardiac muscle such that when P_i reduces force, sufficient cross-bridges remain attached in the vicinity that the activation level is unchanged. Cooperative interactions between cross-bridges and the thin filament regulatory system have been reported in rigor fibers from both cardiac (Martin and Barsotti, 1994) and skeletal fibers (Thirlwell et al., 1994). This cooperativity observed during ATP-induced relaxation of rigor tension in the absence of Ca^{2+} appears to be caused by ADP-bound bridges, and the effects may be more prominent in cardiac muscle because of a higher

affinity for ADP (Martin and Barsotti, 1994). The possibility that ADP-bound rigor bridges prevent thin filament inactivation after caged P$_i$ photolysis in cardiac fibers requires further investigation.

Our data with caged P$_i$ show a clear difference in the interaction of cross-bridges with the thin filament in cardiac versus fast twitch skeletal muscles in actively contraction fibers in the presence of Ca^{2+}. This difference in cooperativity may be responsible for observed differences between cardiac and fast skeletal fibers, such as steepness of steady-state tension-pCa curves (Moss et al., 1986; Araujo and Walker, 1994) and enhanced steepness of tension-pCa curves in the presence of P$_i$ in fast skeletal fibers (Millar and Homsher, 1990) but not in cardiac muscles (Fig. 6; Palmer and Kentish, 1994). The degree of Ca^{2+} sensitivity of tension development rate also differs, increasing 10–15-fold in fast skeletal fibers (Metzger et al., 1989; Araujo and Walker, 1994) but only 4–5-fold in cardiac muscle (Fig. 4; Araujo and Walker, 1994). Finally, the shape of the relationship between tension development rate and activation level, which is approximately linear in cardiac tissues (Fig. 4 B; Araujo and Walker, 1994) and nonlinear in fast skeletal fibers (Brenner, 1988; Metzger et al., 1989; Araujo and Walker, 1994), may also reflect differences in cross-bridge cooperativity. Overall, this difference may contribute to a cardiac system that switches on and off in a more graded manner than does the fast skeletal system.

CONCLUSIONS

The effects of P$_i$ studied either in the steady state or after photorelease from caged P$_i$ were remarkably similar in many ways in ventricular myocytes and fast skeletal fibers. Reversible force generating cross-bridge transitions probed by high P$_i$ in cardiac myocytes were intermediate in rate between slow and fast skeletal fibers. The P$_i$ release step might contribute to the rate limitation in the process of force development in cardiac myocytes, but it is not the rate-limiting step in steady-state ATPase, nor is it the main site of Ca^{2+} regulation. The modulatory effects of Ca^{2+} on P$_i$ release are consistent with reciprocal interactions between force-generating cross-bridges and the thin filament regulatory proteins in cardiac muscle. However, cooperative cross-bridge interactions with the thin filament appear to be different in cardiac myocytes. Whether this is a property of cardiac cross-bridges or cardiac thin filaments (or both) remains to be determined.

REFERENCES

Araujo, A., and J. W. Walker. 1994. Kinetics of tension development in skinned cardiac myocytes measured by photorelease of Ca^{2+}. Am. J. Physiol. 267:H1643–H1653.

Barsotti, R. J., and M. A. Ferenczi. 1988. Kinetics of ATP hydrolysis and tension production in skinned cardiac muscle of the guinea pig. J. Biol. Chem. 263:16750–16756.

Bowater, R., and J. Sleep. 1988. Demembranated muscle fibers catalyze a more rapid exchange between phosphate and ATP than actomyosin subfragment 1. Biochemistry. 27:5314–5323.

Brenner, B. 1988. Effects of Ca^{2+} on cross-bridge turnover kinetics in skinned single rabbit psoas fibers: implications for regulation of muscle contraction. Proc. Natl. Acad. Sci. USA. 85:3265–3269.

Dantzig, J. A., Y. E. Goldman, N. C. Millar, J. Laktis, and E. Homsher. 1992. Reversal of the cross-bridge force-generating transition by photogeneration of phosphate in rabbit psoas muscle fibers. J. Physiol. 451:247–278.

Dantzig, J. A., J. W. Walker, D. R. Trentham, and Y. E. Goldman. 1988. Relaxation of muscle fibers with ATP(γS) and by laser photolysis of caged ATP(γS): evidence for Ca^{2+} dependent affinity of rapidly detaching zero force cross-bridges. Proc. Natl. Acad. Sci. USA. 85:6716–6720.

Ellis-Davies, G. R. C., and J. A. Kaplan. 1994. Nitrophenyl-EGTA, a photolabile chelator that selectively binds Ca^{2+} with high affinity and releases it rapidly on photolysis. Proc. Natl. Acad. Sci. USA. 91:187–194.

Fabiato, A. 1988. Computer programs for calculating total from specified free or free from specified total ionic concentrations in aqueous solutions containing multiple metals and ligands. Methods Enzymol. 157: 378–417.

Glantz, S. A., and Slinker, B. K. 1990. Primer of Applied Regression and Analysis of Variance. McGraw-Hill, New York.

Hibberd, M. G., J. A. Dantzig, D. R., Trentham, and Y. E. Goldman. 1985. Phosphate release and force generation in skeletal muscle fibers. Science. 228:1317–1319.

Hibberd, M. G., and D. R. Trentham. 1986. Relationships between chemical and mechanical events during muscular contraction. Annu. Rev. Biophys. Biophys. Chem. 15:119–161.

Homsher, E., and N. C. Millar. 1990. Caged compounds and striated muscle contraction. Annu. Rev. Physiol. 52:875–896.

Huxley, A. F., and R. M. Simmons. 1971. Proposed mechanism of force generation in striated muscle. Nature. 233:533–538.

Kawai, M., and H. R. Halvorson. 1991. Two step mechanism of phosphate release and mechanism of force generation in chemically skinned fibers of rabbit psoas muscle. Biophys. J. 59:329–342.

Kawai, M., Y. Saeki, and Y. Zhao. 1993. Cross-bridge scheme and kinetic constants of elementary steps deduced from chemically skinned papillary and trabecular muscles of the ferret. Circ. Res. 73:35–50.

Kentish, J. A. 1986. The effects of inorganic phosphate and creatine phosphate on force production in skinned muscles from rat ventricle. J. Physiol. 370:585–604.

Lanzetta, P. A., L. J. Alvarez, P. S. Reinach, and O. A. Candia. 1979. An improved assay for nmole amounts of inorganic phosphate. Anal. Biochem. 100:95–97.

Lu, Z., R. L. Moss, and J. W. Walker. 1993. Tension transients initiated by photorelease of MgADP in skinned skeletal muscle fibers. J. Gen. Physiol. 101:867–888.

Lund, J., M. R. Webb, and D. S. C. White. 1987. Changes in the ATPase activity of insect fibrillar flight muscle during calcium and strain activation probed by phosphate-water oxygen exchange. J. Biol. Chem. 362:8584–8590.

Luo, Y., R. Cooke, and E. Pate. 1993. A model of stress relaxation in cross-bridge systems: effect of a series elastic element. Am. J. Physiol. 267:C1598–C1606.

Martin, H., and R. J. Barsotti. 1994. Relaxation from rigor of skinned trabeculae of the guinea pig by laser flash photolysis of caged ATP. Biophys. J. 66:1115–1128.

Matsubara, I., D. W. Maughan, Y. Saeki, and N. Yagi. 1989. Cross-bridge movement in rat cardiac muscle as a function of calcium concentration. J. Physiol. (Lond.). 417:555–565.

Metzger, J. M., M. L. Greaser, and R. L. Moss. 1989. Variation in cross-bridge attachment rate and tension with phosphorylation of myosin in mammalian skinned skeletal muscle fibers. J. Gen. Physiol. 98:855–883.

Millar, N. C., and E. Homsher. 1990. The effect of phosphate and calcium on force generation in glycerinated rabbit skeletal muscle fibers. J. Biol. Chem. 265:20234–20240.

Millar, N. C., and E. Homsher. 1992. Kinetics of force generation and phosphate release in skinned rabbit soleus muscle fibers. *Am. J. Physiol.* 262:C1239–C1245.

Moss, R. L., M. R. Lauer, G. G. Giullian, and M. L. Greaser. 1986. Altered Ca^{2+} dependence of tension development in skinned skeletal muscle fibers following modification of troponin by partial substitution with cardiac troponin C. *J. Biol. Chem.* 261:6096–6099.

Palmer, S., and J. C. Kentish. 1994. The role of troponin C in modulating the Ca^{2+} sensitivity of mammalian skinned cardiac and skeletal muscle fibers. *J. Physiol.* 480:45–60.

Pate, E., and R. Cooke. 1989. Addition of phosphate to active muscle probes actomyosin states within the power stroke. *Pflugers Arch.* 414:73–81.

Song, Q., A. Araujo, and J. W. Walker. 1996. Kinetics of activation and P_i release in cardiac myocytes using caged P_i and caged Ca^{2+}. *Biophys. J.* 70:A170. (Abstr.)

Thirlwell, H., J. E. T. Corrie, G. P. Reid, D. R. Trentham, and M. A. Ferenczi. 1994. Kinetics of relaxation from rigor of permeabilized fast-twitch skeletal fibers from the rabbit using a novel caged ATP and apyrase. *Biophys. J.* 67:2436–2447.

Walker, J. W., Z. Lu, and R. L. Moss. 1992. Effects of Ca^{2+} on the kinetics of phosphate release in skeletal muscle. *J. Biol. Chem.* 267:2459–2466.

Webb, M. R., M. G. Hibberd, Y. E. Goldman, and D. R. Trentham. 1986. Oxygen exchange between P_i in the medium and water during ATP hydrolysis mediated by skinned fibers from rabbit psoas muscle: evidence for P_i binding to a force generating state. *J. Biol. Chem.* 261:15557–15564.

White, H. D., and E. Taylor. 1976. Energetics and mechanism of actomyosin adenosine triphosphatase. *Biochemistry.* 15:5818–5826.

Wolff, M., K. MacDonald, and R. L. Moss. 1995. Rate of tension development in cardiac muscle varies with level of activator calcium. *Circ. Res.* 76:154–160.